Tampereen yliopisto

Laura Pellinen

SYNDEKAANI-4 KOKEELLISESSA IHOSYÖPÄMALLISSA

Lääketieteen ja terveysteknologian tiedekunta

Syventävien opintojen kirjallinen työ

Tammikuu 2020

TIIVISTELMÄ

Laura Pellinen: Syndekaani-4 kokeellisessa ihosyöpämallissa
Syventävien opintojen kirjallinen työ
Tampereen Yliopisto
Lääketieteen lisensiaatin tutkinto-ohjelma
Tammikuu 2020

Syndekaanit ovat solukalvon heparaanisulfaatti-proteoglykaaneja, jotka toimivat ko-reseptoreina kasvutekijöille, sytokiineille ja morfogeeneille ja ovat tärkeitä solunsisäisessä signaloinnissa. Niitä on lähes jokaisen solutyypin pinnalla ja ne säätelevät niin normaalien kuin patologistenkin tilojen kehitystä.

Syndekaaneja on neljää eri tyyppiä, joista syndekaani-4 toimii tärkeänä säätelijänä solujen migraatiossa. Sitä esiintyy eniten fibroblastien ja epiteelisolujen pinnalla. Syndekaani-4 säätelee fysiologista kudosten paranemista ja angiogeneesiä, mutta myös patologista tuumorikasvua.

Syndekaani-4:sta koodaava SDC4-geeni on yhdistetty useisiin ihmisten syöpiin, mutta sen vaikutuksesta tuumorin muodostumisessa ja kasvussa ei ole suoraa näyttöä. ”Syndekaani-4 kokeellisessa ihosyöpämallissa”- tutkimuksen tarkoitus oli selvittää SDC4:n vaikutusta tuumorikasvuun ihon epidermaalisessa karsinogeenimallissa.

Tutkimuksessa käytettiin SDC4-poistogeenisiä sekä villityypin hiiriä, joiden selkä käsiteltiin ensin karsinogeenillä (DMBA) ja sitten kahdesti viikossa 21 viikon ajan kasvua kiihdyttävällä aineella (TPA). Syntyneet papilloomat laskettiin ja niiden koko ja kasvu mitattiin tarkasti.

SDC4-geenin poisto ei vaikuttanut siihen, kuinka nopeasti papilloomia alkoi kehittymään. Poistogeenisillä hiirillä ilmeni kuitenkin neljä kertaa vähemmän papilloomia ja ne olivat kymmenen kertaa pienempiä kuin villityypin hiirillä.

Tutkimus osoittaa, että SDC4-geenillä on merkittävä rooli tuumorikasvussa.

Avainsanat: tuumorikasvu, solumigraatio, solusignalointi

Sisällys

1 SYNDEC1AN-4 PROMOTES TUMOR GROWTH IN CARCINOGEN-INDUCED SKIN CANCER MODEL

1.1 Abstract

The *syndecan-4* (SDC4) gene encodes transmembrane heparan sulfate proteoglycans that act as receptors for extracellular matrix molecules and co-receptors for growth factors, cytokines, and morphogens. Despite the SDC4 been implicated for promoting tumour progression in wide variety of different human cancers, no direct evidence on its role in tumour progression exists. Using mice with a deletion of the *SDC4* gene (SDC KO), we found that SDC4 facilitates DMBA/TPA-induced skin tumour growth. The tumours appeared in wild-type (WT) mice at the same rate as in SDC4 KO mice, but WT mice developed almost 4 times more tumours and almost 10 times more large papillomas than SDC4 KO mice. We provide first direct evidence that SDC4 is indeed needed for tumor growth by showing that it is pro-tumourigenic in the DMBA/TPA tumour model.

1.2 Introduction

Syndecans are transmembrane heparan sulfate proteoglycans that act as receptors for extracellular matrix (ECM) molecules and co-receptors for growth factors, cytokines, and morphogens (1-3). They are present in almost all cell types and tissues and they act as regulators not only in normal but also in pathological conditions (1-3). There are four vertebrae syndecans (SDCs), SDC1-4, each with large heparan sulfate and

chondroitin sulfate chains covalently attached to the extracellular domain and short cytoplasmic tails that interact with a number of signaling adaptors and enzymes (1-3). The fibronectin receptor syndecan-4 (SDC4) regulates GTPase activity and adhesive function to modulate cell migration (4,5). It is ubiquitously expressed, most notably in fibroblast, and its defect leads to impaired wound healing due to migration and angiogenesis defects (5-7).

The heparan sulfate (HS) side chains of the SDCs bind to a plethora of proteins, including chemokines and cytokines (~60) and growth factors and morphogens that play essential roles in cancer progression and tissue repair (~50); blood coagulation factors such as serine proteases and their inhibitors (~25); structural ECM proteins such as collagens, fibronectin, and vitronectin (~25); proteins involved in the complement pathways (~20); single-transmembrane signaling receptors (~15); and cell adhesion proteins (~10) (2). The interaction of SDCs with growth factors and their respective receptors has been characterized in great detail (1-3). Because of the high negative charge in HS side chain of the SDCs, the initial contact heparin binding growth factors make with the cells is by binding to the HS chains (1-3). The HS chain acts as a template that bridges growth factor and its receptor together. Formation of the complex effectively lowers the concentration of growth factor required to initiate signalling through its receptor and extends the duration of the response (1-3). Thus, it is not striking that SDCs have been implicated to regulate not only the physiological tissue repair but also the pathological tumour growth (3,5,8).

Due to its essential role in mediating the growth stimulatory signal provided by multiple growth factors and its rapid expression at the onset of tumor formation in various forms of cancer (1-3,5,8), SDC4 has been implicated in the pathogenesis of wide variety of human cancers (8). However, there is no direct evidence that SDC4 indeed promotes tumour formation (8), a point highlighted by the fact that the redundancy of an individual SDC gene has no critical role during development (6,7). Thus, we decided to study whether carcinogen-initiated tumour formation is

dependent of SDC4 by exploring the role of SDC4 in a skin epidermal carcinogenesis model (two-stage DMBA/TPA model) in wild-type (WT) and SDC4 knockout mice (SDC4 KO).

1.3 Methods

1.3.1 Mice

The generation of syndecan-4 mice have been described in detail elsewhere (7). The mice were obtained from the laboratory of Mark Bass (University of Bristol, Bristol, UK). Before any experiments, syndecan-4 KO mice were backcrossed eight generations with C57BL/6 strain (Harlan) to obtain syndecan-4 expressing (wild-type, WT) and syndecan-4 KO strain in the same background genetic strain of mice (littermates). Then homozygous syndecan-4 KO animals were bred. The genotype was determined in each animal by PCR. Mice were fed with standard laboratory pellets and water *ad libitum*. All animal experiments were performed in accordance with protocols approved by the National Animal Ethics Committee of Finland.

1.3.2 Skin tumour induction

Syndecan-4 KO and C57BL/6 WT mice were treated with DMBA and TPA to induce skin tumours according to the established protocol (9,10). In brief, the backs of 8-week-old mice were shaved and 24h later 50 µg DMBA (7,12-Dimethylbenz[a]anthracene) (Sigma, Dorset, UK) in 200 µl acetone was applied topically on the shaved area of the dorsal skin. After a week, the back skin of the mice was treated twice a week with 5 µg TPA (12-*O*-tetradecanoylphorbol-13-acetate) (Sigma) in 200 µl acetone for 21 weeks (10). Tumours (1 mm in diameter or larger) were counted twice a week. The fur excluding tumours was carefully shaved every two weeks.

1.3.3 Immunohistochemical (IHC) and TUNEL staining

Samples of back skin from sacrificed, shaved control mice or mice at week 21 of the tumour induction experiment were collected and fixed with 4% paraformaldehyde and embedded in paraffin according to standard protocols. Hematoxylin/eosin staining and DAB immunohistochemical staining (IHC) was performed on 6 µm thick paraffin sections. The IHC stainings were carried out essentially as described previously (10). Briefly, the following primary antibodies were used for IHC (according to the manufacturer's instructions): M7249 TEC-3 rat anti-Ki67 and A0452 rabbit anti-CD3 (DakoCytomation, Glostrup, Denmark), 550274 rat anti-CD31 (BD Pharminogen, Oxford, UK), 68672 rabbit anti-neutrophil elastase (AbCam, Cambridge, UK) and MF48000 BM8 rat anti-F4/80 (Life Technologies Ltd., Paisley, UK) (10). The blocking reagents used for IHC were S2O23 REAL and S0809 Antibody Diluent (Dako). In the case of blocking prior to CD3 or neutrophil elastase staining, G9023 goat serum or A4503 BSA (Sigma) were used respectively, at 5% in PBS. The horseradish peroxidase (HRP) conjugated secondary antibody reagents used were: PO448 goat anti-rabbit (Dako), 414311F anti-rat Histofine (Nichirei Bio, Tokyo, Japan) and for neutrophil elastase staining RMR622 Rabbit on Rodent (Biocare Medical, Concord, CA, USA). XMF963 XM-Factor (Biocare) was used to block before secondary staining with Rabbit on Rodent. Peroxidase reactive chromogens used were K3465 DAB (DAKO) and RAEC810 Romulin AEC (BioCare). Immunohistochemical TUNEL staining for apoptotic nuclei was performed using the K403-50 TUNEL IHC Kit (Biovision, Milpitas, CA, USA) with Methyl Green nuclear counter stain, as described previously (10).

1.3.4 Quantitative analysis of immunostaining and histochemical staining

All slides were scanned using the Aperio ScanScope® CS and XT systems (Aperio Technologies Inc., California, USA) (10,18). Slides were viewed and analysed

remotely using desktop personal computers employing the web-based ImageScope™ viewer. The Spectrum digital pathology system analysis algorithm package and Image Scope analysis software (version 9; Aperio Technologies Inc.) were applied to quantify immunohistochemical signal. These algorithms calculate the area of positive staining, the average positive intensity (optical density), as well as the percentage of weak (1+), medium (2+), and strong (3+) positive staining (10,18). All quantified histochemical analyses (Ki-67, CD31, F4/80, CD3, TUNEL and M2-macrophages) were performed according to the protocols used to established these algorithms for each respective staining (10,18).

1.3.5 Flow cytometry

The skin draining lymph nodes (dLN) and spleens were collected immediately after the sacrifice of the animal and tissues were placed in ice-cold PBS. For surface markers, the dLN and spleen cells were stained with antibodies against mouse CD4, CD8, CD44, CD62L and CD69 (all from eBioscience). For intracellular staining, isolated dLN cells were stimulated with PMA and Ca-ionomycin for 4 hours, and Brefeldin A and Monensin were applied for the last 2 hours of the stimulation. The cells were stained with surface markers and subsequently fixed overnight with Fixation/Permeabilization solution (from Foxp3/Transcription Factor Staining Buffer Set, eBioscience), permeabilized with Permeabilization Buffer (eBioscience) and stained with intracellular antibodies (IL-10, IFNγ, IL-17A, Foxp3; all from eBioscience), according to the manufacturer's instructions. All cells were analysed with FACSCanto II (Becton Dickinson) instrument. Data analysis was performed with FlowJo software (Flowjo LLC, Ashland, OR, USA).

1.3.6 Statistical analysis

Mean averages are shown with 95% confidence intervals. All data were analysed to determine if it was normally distributed (D'Agostino & Pearson omnibus and

Shapiro-Wilk normality tests). Significance at a given time point was calculated by two-tailed Student's *t*-test for normally distributed data. An alpha level less than 0.05 was considered significant. Survival plot data were analysed by log-rank (Mantel-Cox) test and non-normally distributed time course data were analysed by non-linear regression. Prism 6 (GraphPad Software, La Jolla California, USA) was used for a majority of the analyses and STATA 13 (StataCorp LP, College Station, Texas, USA:) statistical analysis software was used for non-linear regression analysis, as indicated.

1.4 Results

1.4.1 SDC4 plays an important role in skin tumour growth

To investigate the role of SDC4 in skin tumour formation, we treated the back skin of adult mice deficient for *SDC4* gene expression (SDC4 KO) and wild-type mice (WT, as control) once with a local application of the mutagen DMBA, and then repeatedly with the growth-promoting TPA, twice weekly for a period of 21 weeks. This treatment induces papillomas derived from the interfollicular epidermis (9,10).

The first papillomas were observed both in the WT and SDC4 KO mice 9 weeks after the beginning of the DMBA/TPA treatment, and after 12 and 13 weeks, none of the animals were tumour-free (Figure 1a). No difference was detected in the "tumour-free" survival time between SDC4 KO and WT mice (Figure 1a). However, the tumours were incident in SDC4 WT animals at a rate on average threefold greater than in KO mice during the course of experiments (negative binominal regression analysis: incidence rate ratio (IRR)= 0.00; 95% confidence interval (CI) 0.00, 0.00). At the end of the experiments (21 weeks of DMBA/TPA treatment), SDC4 WT

animals had on average almost 3.5 times more tumours than the KO mice (Figure 1a-d). Furthermore, majority of tumours grew into large papillomas (> 2 mm in size) in SDC4 WT mice, whereas the large papillomas were very rare in SDC4 KO mice (Fig.). Almost 10-fold more large papillomas were identified in the SDC4 WT than in the KO mice (Fig.).

1.4.2 SDC4 expression is …..

We confirmed the total lack of SDC4 protein in the SDC4 KO mice by immunohistochemistry both in untreated and DMBA/TPA-treated skin samples (Figure 2a). We detected very strong expression of SDC4 protein in the epidermal cell layer either in untreated or DMBA/TPA-treated WT mice (Figure 2b). Blood vessels also expressed SDC4 protein in the WT….

1.4.3 The resistance of R-Ras KO mice to skin tumourigenesis is not associated with decreased vascularisation

To understand the mechanism of the tumour-promoting function of R-Ras in the skin, we continued to analyse the whole skin by determining the epidermal and dermal thickening, and the amount of vasculature (angiogenesis) in the back skin of DMBA/TPA treated and untreated mice. All analyses were performed from the same part of the back skin in all animals to avoid any bias (such as selecting a plane of analyses to go through tumour).

In untreated mice, loss of SDC4 had minor effects on epidermal and dermal thicknesses, as the SDC4 KO mice had a slightly thinner epidermis and thicker dermis than the WT littermates ($P <$ and $P <$ respectively, Supplementary Figure S2). Treatment with DMBA/TPA induced a substantial increase ($P < 0.001$) and approximate doubling in both dermal and epidermal thickness in both genotypes; both epidermis ($P <$) and dermis (not significant) being apparently substantially

thicker in the WT mice (the analysis was performed only from areas devoid of papillomas) than in the SDC4 KO mice (Supplementary Figure S2).

As the availability of vascular supply is a limiting factor for tumour growth and SDC4 is implicated in processes involving vascular defects in fetal placental labyrinth and poor angiogenic response in postnatal wound healing (6).

1.4.4 Skin draining lymph node and spleen T cell populations are not different between SDC4 KO and WT mice

To gain more information on the T lymphocyte (helper, cytotoxic or regulatory T cells; memory and activation status), myeloid and B cell populations, the skin draining lymph node (dLN) and spleen cells from SDC4 KO mice and their WT littermate controls were subjected to flow cytometric analysis after the 21-week DMBA/TPA treatment. CD4+ (T helper cells) and B cells are known to be crucial for the development of tumours in DMBA/TPA-model (11,12), whereas CD8+ (Cytotoxic T cells) cells inhibit the tumour development in the model (11). There were no differences in any of the analysed T cell, myeloid or B cell populations in the spleen (Fig.). There were no significant differences in the total CD4+ and CD8+ T cell percentages (of total live cells) in the dLNs between the SDC4 KO and WT mice treated with DMBA/TPA for 21 weeks (Fig.) Then we analysed the memory phenotypes (central memory T cells, effector memory T cells, naïve T cells) of spleen and dLN T cells by using CD44 and CD62L antibodies and flow cytometry. There were no differences in the different memory T cell populations in the spleen (Fig.), but there were substantially more both CD4+ $CD62L^{low}CD44^{high}$ (P=0.057; not significant), CD8+ $CD62L^{low}CD44^{high}$ (P=0.017) as well as slightly more CD8+ $CD62L^{high}CD44^{high}$ (P=0.069; not significant) cells in the dLNs in the SDC4 KO than in the WT mice (Fig.). However, there were no differences in the number of recently activated T cells, as the same proportion of both CD4+ and CD8+ T cells from the KO and the WT animals were positive for CD69 (Fig.). Neither were there were any

differences identified in myeloid or B cell populations in the dLNs between SDC4 WT and KO mice (Fig.).

The percentage of regulatory T cells (Tregs) was assessed by staining the dLN cells with antibodies against CD25 and Foxp3, and performing flow cytometric analysis. There were no differences in the number of Treg cells in the dLNs of SDC4 KO mice compared to those of WT littermates from mice treated with DMBA/TPA for 21 weeks (Fig. 3).

In conclusion, the treatment of mice with DMBA/TPA for 17 weeks does not have an effect on the numbers of the skin draining lymph node T cells, although….

1.4.5 No differences in the T cell-derived tumour promoting cytokines during tumour development

It is an established fact that tumourigenesis in the DMBA/TPA model is highly dependent upon the induction of acute inflammation (13). To investigate tumour promoting cytokine production of T cells in the tumour development in the SDC4 KO mice, we analysed dLN T cells by intracellular staining and flow cytometry. We focused on pro-inflammatory interferon gamma (IFNγ) and interleukin (IL) 17A (IL-17A) and IL-10. Both IFNγ and IL-17A, in particular, are known to be pro-tumourigenic in the DMBA/TPA model (14-17) and inflammatory cell produced IL-10 has been implicated in the pathogenesis of the model (11). There were no differences in the percentage of CD8+, Tregs nor CD4+ effector cells producing IFNγ and IL-17A in the dLNs of SDC4 KO and WT mice and there was no difference in the production of CD4+ T cell-produced IL-10 (Fig.).

1.5 Discussion

In summary, our study shows an important role of the SDC4 in epidermal hyperplasia and tumour growth in a skin carcinogenesis-tumour model. Our finding is novel in the sense that SDC4 has not been directly shown to promote tumour progression previously (Figure 2). Our finding is also somehow an unexpected outcome, as SDC4 has so far been redundant in majority of biological processes in has been studied (7).

On the other hand, SDC4 is an important receptor for large number of heparin binding growth factors that are crucial for tumour growth. One could also make an argument that is kind of natural that a lack of important receptor for large number of cytokines, chemokines and growth factors should inhibit the progression of cancer in the model that requires large variety of such diverse biological processes as inflammation, angiogenesis, migration and transformation to be involved for tumours to grow.

1.6 References

(1) Bishop JR, Schuksz M, Esko JD. Heparan sulphate proteoglycans fine-tune mammalian physiology. Nature 2007 Apr 26;446(7139):1030-1037.

(2) Xu D, Esko JD. Demystifying heparan sulfate-protein interactions. Annu Rev Biochem 2014;83:129-157.

(3) Bass MD, Morgan MR, Humphries MJ. Syndecans shed their reputation as inert molecules. Sci Signal 2009 Mar 31;2(64):pe18.

(4) Bass MD, Williamson RC, Nunan RD, Humphries JD, Byron A, Morgan MR, et al. A syndecan-4 hair trigger initiates wound healing through caveolin- and RhoG-regulated integrin endocytosis. Dev Cell 2011 Oct 18;21(4):681-693.

(5) Morgan MR, Hamidi H, Bass MD, Warwood S, Ballestrem C, Humphries MJ. Syndecan-4 phosphorylation is a control point for integrin recycling. Dev Cell 2013 Mar 11;24(5):472-485.

(6) Echtermeyer F, Streit M, Wilcox-Adelman S, Saoncella S, Denhez F, Detmar M, et al. Delayed wound repair and impaired angiogenesis in mice lacking syndecan-4. J Clin Invest 2001 Jan;107(2):R9-R14.

(7) Ishiguro K, Kadomatsu K, Kojima T, Muramatsu H, Tsuzuki S, Nakamura E, et al. Syndecan-4 deficiency impairs focal adhesion formation only under restricted conditions. J Biol Chem 2000 Feb 25;275(8):5249-5252.

(8) Barbouri D, Afratis N, Gialeli C, Vynios DH, Theocharis AD, Karamanos NK. Syndecans as modulators and potential pharmacological targets in cancer progression. Front Oncol 2014 Feb 3;4:4.

(9) Perez-Losada J, Balmain A. Stem-cell hierarchy in skin cancer. Nat Rev Cancer 2003 Jun;3(6):434-443.

(10) May U, Prince S, Vähätupa M, Laitinen AM, Nieminen K, Uusitalo-Järvinen H, et al. Resistance of R-Ras knockout mice to skin tumour induction. Sci Rep 2015 Jul 2;5:11663.

(11) Yusuf N, Nasti TH, Katiyar SK, Jacobs MK, Seibert MD, Ginsburg AC, et al. Antagonistic roles of CD4+ and CD8+ T-cells in 7,12-dimethylbenz(a)anthracene cutaneous carcinogenesis. Cancer Res 2008 May 15;68(10):3924-3930.

(12) Schioppa T, Moore R, Thompson RG, Rosser EC, Kulbe H, Nedospasov S, et al. B regulatory cells and the tumor-promoting actions of TNF-alpha during squamous carcinogenesis. Proc Natl Acad Sci U S A 2011 Jun 28;108(26):10662-10667.

(13) Swann JB, Vesely MD, Silva A, Sharkey J, Akira S, Schreiber RD, et al. Demonstration of inflammation-induced cancer and cancer immunoediting during primary tumorigenesis. Proc Natl Acad Sci U S A 2008 Jan 15;105(2):652-656.

(14) He D, Li H, Yusuf N, Elmets CA, Athar M, Katiyar SK, et al. IL-17 mediated inflammation promotes tumor growth and progression in the skin. PLoS One 2012;7(2):e32126.

(15) Reiners JJ,Jr, Rupp T, Colby A, Cantu AR, Pavone A. Tumor copromoting activity of gamma-interferon in the murine skin multistage carcinogenesis model. Cancer Res 1989 Mar 1;49(5):1202-1206.

(16) Wang L, Yi T, Zhang W, Pardoll DM, Yu H. IL-17 enhances tumor development in carcinogen-induced skin cancer. Cancer Res 2010 Dec 15;70(24):10112-10120.

(17) Xiao M, Wang C, Zhang J, Li Z, Zhao X, Qin Z. IFNgamma promotes papilloma development by up-regulating Th17-associated inflammation. Cancer Res 2009 Mar 1;69(5):2010-2017.

(18) Järvinen TA, Ruoslahti E. Target-seeking antifibrotic compound enhances wound healing and suppresses scar formation in mice. Proc Natl Acad Sci U S A 2010 Dec 14;107(50):21671-21676.

2 VEGFA-driven pathological angiogenesis requires the proteoglycan syndecan-4 or Syndecan-4 provides an essential signaling checkpoint in pathological angiogenesis

2.1 Abstract

Angiogenesis is a hallmark and exacerbating factor in cancer and neovascular eye diseases. Significant efforts have been made to control this process for therapeutic benefit, most notably by targeting the key angiogenic growth factor, vascular endothelial growth factor-A (VEGFA) and its receptor VEGFR2. Here, we report a new fundamental role for Syndecan-4 (SDC4) in VEGFA-driven pathological neovascularisation. The SDC4 null mouse (*Sdc4*-/-) exhibited reduced tumorigenesis and delayed wound healing in the eye due to impaired angiogenesis. We establish that this results from a failure to respond to VEGFA, and demonstrate that SDC4 is required for VEGFR2 signalling. We further show that blockade of VEGFA-driven neovascularisation can be achieved using a soluble form of SDC4. These findings establish a molecular framework coupling SDC4 with pathological angiogenesis, which may prove significant for the development of future anti-angiogenic therapeutic applications.

2.2 Main text

The formation of new blood vessels from pre-existing ones (angiogenesis) is a critical developmental process and is an important component of physiological tissue regeneration[1]. In cancer, inflammatory disorders and neovascular eye diseases, angiogenesis is a key feature in the pathogenesis and significant efforts have been made to control this process for therapeutic benefit[2-5]. The pro-angiogenic chemokine vascular endothelial growth factor A (VEGFA) and its receptor VEGFR2 are the major drivers of angiogenesis in these pathologies and drugs targeting this axis have been used with substantial success in the clinic. However, there are issues of patient non-response, resistance to therapy and several side effects that are associated with

VEGFA/VEGFR2 targeting drugs[6, 7], highlighting the need for better understanding of the underlying molecular basis of pathological angiogenesis.

There is considerable evidence to suggest a role for heparan sulfate proteoglycans (HSPGs) in VEGFA signaling. HSPGs are abundant cell surface and matrix molecules that influence cell responses to growth factors as well as the distributions of chemokines and morphogens in tissues [8, 9]. VEGFA binds to heparan sulfate (HS) with high affinity[10], and cells where HS has been enzymatically removed have abrogated VEGFA signalling[11]. VEGFR2 also binds to HS, suggesting that HSPGs may facilitate the formation of an active signalling complex[12]. Thus, HSPGs are implicated as important co-receptors and regulators of VEGFA gradients. The interaction between VEGFA and HSPGs is largely through the glycosaminoglycan part of the molecule[10, 11] though the identity and the role of a specific HSPG core protein has remained elusive. The syndecans are a four-member family of transmembrane HSPGs with diverse roles in cell adhesion, receptor trafficking and growth factor signalling[13, 14]. Roles in angiogenesis have also been proposed; for example, regulatory sequences in both the syndecan-1 and -2 ectodomains can inhibit this process via distinct pathways[15-17]. Syndecan-4 null mice (*Sdc4-/-*) exhibit defects in the development of the foetal labyrinth and in granulation tissue formation after wounding[18, 19] which is suggestive of a role in new blood vessel formation. We have therefore investigated whether an individual HSPG has a role in disease models where angiogenesis is a feature.

2.2.1 *Sdc4-/-* animals are protected in tumor models by reduced angiogenesis

The formation of new blood vessels is an essential component of tumor growth and progression[20] and we observed that in a skin epidermal carcinogenesis model (two stage DMBA/TPA), tumor incidence and size were greatly reduced in *Sdc4*-/- mice compared to wild-type (WT) animals, although the tumor-free survival was almost identical (**fig. S1**). WT animals had considerably more papillomas (2.3x) than *Sdc4-/-* mice at the end of the experiment (week 19) and, in particular, larger tumors (> 2 mm)

were significantly more prevalent in WT animals (**Fig. 1A-C**). To dissect whether this phenotype is due to *Sdc4*-/- tumor cells or *Sdc4-/-* tumor vasculature, we injected B16F1 melanoma cells, which express SDC4 (**fig. S2A**), into the flank of WT and *Sdc4-/-* mice. Mice were sacrificed after 2 weeks and both tumor volume and weight were greatly reduced in *Sdc4*-/- animals when compared to WT controls (**Fig. 1D and E, fig. S2C and D**). This suggested that tumor angiogenesis was compromised in *Sdc4-/-* mice.

A recent study using a Lewis lung carcinoma model concurred with our findings that tumor volume was greatly reduced in in *Sdc4-/-* animals but correlated with an increased number of Natural killer (NK) cells in immune infiltrates from tumors[21]. This prompted us to analyze the immune infiltrates from B16F1 tumors and spleens from healthy mice. This revealed no differences in the number of NK cells between WT and *Sdc4-/-* animals (**Fig. 1F and G**) and this was also true of other leukocytes subsets including B cells, T cells, monocytes and neutrophils (**fig. S3A and B**). Analysis of skin and tumors from the DMBA/TPA model also showed no trend for differential inflammatory responses, i.e. macrophages, T cells or neutrophils, between WT and *Sdc4-/-* animals (**fig. S4A-F**).

Importantly, histological analysis of B16F1 tumor sections from WT animals revealed vascular structures with, in many cases, a well-defined lumen (white arrows in **Fig. 1H**). In *Sdc4*-/- mice-derived tumors, endothelial cells (ECs) failed to organize into tubules and were more sparsely distributed (**Fig. 1H and I**). These observations led us to conclude that the reduced tumor growth in *Sdc4-/-* mice was primarily a result of defective tumor vascularization and not due to any inherent differences between WT and Sdc4-/- mouse immune responses.

2.2.2 Pathological angiogenesis in the eye is impaired in *Sdc4-/-* animals

Having established that tumor angiogenesis was impaired in *Sdc4-/-* mice, we next tested whether other pathological angiogenic responses were affected in these animals.

Oxygen-induced retinopathy (OIR) is a pure hypoxia-driven, VEGFA-dependent angiogenesis-model that recapitulates features of diabetic retinopathy, whereas, laser-induced choroidal neovascularization (CNV) models neovascular ('wet') age-related macular degeneration[22]. OIR was performed on 7 day old WT and *Sdc4*-/- pups by exposing them to hypoxia (75 % O_2 for 5 days) leading to the abolition of the retinal vasculature, before being returned to normoxia which stimulates a neovascular response. After 5 days in normoxic conditions the formation of neovascular tufts (pathological angiogenesis) was greatly reduced (~40%) in retinas of *Sdc4*-/- mice compared to WT mice (**Fig. 2A and B, fig. S5A-D**). Laser photocoagulation was performed on eyes of WT and *Sdc4*-/- littermates to stimulate a neovascular response in the choroid. Areas of CNV measured 7 days after injury by fluorescein angiography were significantly smaller in the eyes of *Sdc4*-/- mice (~75%, by lesion area) (**Fig. 2C and D**). Lesions were predominantly composed of ECs on the basis of BS1-isolectin staining (**fig. S6A and B**).

We confirmed that the defects in this model were the result of impaired angiogenesis in an *ex vivo* model of CNV where explants of choroid/RPE tissue from WT, *Sdc4*+/- and *Sdc4*-/- littermates were in embedded collagen I and exposed to VEGFA. Significantly more angiogenic sprouts emerged from WT explants compared to *Sdc4*-/- explants (**Fig. 2E and F**). Explants from the heterozygote (*Sdc4*+/-) mice exhibited an intermediate phenotype indicating that the angiogenic response associated with SDC4 is subject to gene dosage effects. This was corroborated using the aortic ring model of angiogenesis which also showed very limited angiogenic sprouting in *Sdc4*-/-, and *Sdc4*+/- rings compared to WT controls (**Fig. 2G**). Notably, the few sprouts formed in the *Sdc4*-/- explants were immature as shown by reduced pericyte coverage (**Fig. 2H**). Together these data indicate that pathological angiogenic responses in the *Sdc4*-/- mouse are impaired.

2.2.3 SDC4 is upregulated during pathological angiogenesis

Sdc4-/- mice develop normally and show no gross abnormalities[19], however, no detailed studies have been carried out to assess whether vasculogenesis in *Sdc4*-/- mice culminates in a normal vascular network comparable to that of WT littermates. During the early stages of murine postnatal development angiogenesis occurs in the eye leading to the formation of a superficial retinal vascular plexus. In C57BL6 mice this occurs during the first 8 days after birth. We compared the retinal vasculature of WT, *Sdc4*+/- and *Sdc4*-/- neonates at P6 and observed no differences in terms of vessel extension (**Fig. 3A and B**). Although we observed a slight reduction in vascular area coverage, there was no difference in the number of arteries or veins in *Sdc4-/-* mice (**Fig. 3C and D, fig. S7A and B)**. Moreover, no morphological differences were apparent in the microvasculature of skin, muscle or connective tissue between *Sdc4*-/- and WT adult animals (**fig. S7C and D**) and this was also reflected in an analysis of vessel heterogeneity (**fig. S7D**), vessel density (**fig. S7E**), pericyte coverage (**fig. S7F**) and vascular area in the choroid membranes (**fig. S7G**). Furthermore, vascular functionality, as measured by increased permeability in response to the vasodilator Bradykinin, was also unaffected in *Sdc4-/-* adult animals compared to WT mice (**fig. S7H**). These data suggest that *Sdc4-/-* mice do not exhibit any adverse phenotype associated with vascular development or function. To explore this further, we determined whether SDC4 expression was regulated during this process by measuring syndecan family gene expression during the development of retinal vasculature, comparing this profile to a situation where angiogenesis occurs in a pathological setting (hypoxia-induced, VEGFA-driven model). We performed quantitative rtPCR on retinas from P0, 4, 7, 12 and 17 neonates to measure expression of syndecans-1, -2, -3 and -4. SDC4 gene expression remained constant in these samples (**Fig. 3E**). When pups were subjected to OIR we saw a marked increase in SDC4 gene expression in retinas in which neovascularization was occurring in P17 pups, when compared to the other 3 syndecans whose expression remained stable during the induction of angiogenesis (**Fig. 3F**).

To address the relevance of our findings on the role of SDC4 on pathological angiogenesis to human disease, the pathological retinal neovascular membranes that develop in human diabetic retinopathy patients were studied. Neovascular membranes were collected from patients suffering from type I diabetes, who had already developed tractional retinal detachment due to fibrosis. These samples represent the end stage of the disease, but still contain regions with active pathological angiogenesis. In the diabetic neovascular membranes SDC4 expression was evident mainly in blood vessels (**fig. S8A**). Double-staining of human tissue samples for SDC4 and either VEGFR2 (a marker of pathological immature blood vessels) or CD31 (a general marker of blood vessels) revealed that SDC4 expression was a feature of vessels which were also expressing VEGFR2 and not a general characteristic of the blood vessels in these samples (**fig. S8A-C**). This suggests a close association between SDC4 and VEGFR2 on newly formed vessels in diabetic retinopathy.

These data indicate that SDC4 is upregulated in response to pathological stimuli leading to neovascularization, but not during normal development of the retinal vasculature. To further investigate this hypothesis, we stimulated isolated primary murine ECs (MLECs) with the angiogenic factors VEGFA, bFGF and angiopoietin-2 before measuring SDC4 expression. This analysis revealed a time-dependent upregulation of SDC4 gene transcription in response to bFGF and angiopoietin-2, indicating that SDC4 is upregulated in angiogenic scenarios on ECs (**Fig. 3G**). Immunofluorescence analysis on mature venules and arterioles revealed minimal SDC4 expression on the endothelium (**fig. S9A-E**). However, SDC4 was highly expressed on *ex vivo* angiogenic sprouts both on ECs (counter-stained with BS1-isolectin) and stromal cells, possibly pericytes and smooth muscle cells, suggesting that SDC4 is upregulated on blood vessels during angiogenesis (**Fig. 3H**).

2.2.4 SDC4 is involved in angiogenic responses to VEGFA

The principal driver of angiogenesis in the models described above is VEGFA[7, 23] and we speculated that the angiogenesis defects observed in *Sdc4*-/- animals may be the result of impaired responsiveness to this protein. Therefore, WT and *Sdc4*-/- mice were injected with Matrigel containing VEGFA and bFGF in combination or separately. All 3 conditions triggered an angiogenic response in WT mice as evidenced by plug vascularity. *Sdc4*-/- mice exhibited an identical response to bFGF but angiogenesis was not induced by VEGFA (**Fig. 4A and 4B**). This attenuated angiogenic response to VEGFA was confirmed using the aortic ring assay where new blood vessel sprouting was abolished in *Sdc4*-/- aortic rings in response to VEGFA but not bFGF (**Fig. 4C and D**). These data suggest that *Sdc4*-/- mice have a specific defect in their response to VEGFA-driven angiogenesis.

We assessed whether SDC4 had a key role in VEGFA/VEGFR2 signaling in ECs. First, a proximity ligation assay was used to investigate whether SDC4 and VEGFR-2 associated in a complex in ECs following VEGFA treatment. Confluent WT MLECs were treated with 30 ng/ml of VEGFA for 2 min or 5 min. Within 2 min of VEGFA treatment, SDC4/VEGFR2 complexes appeared on ECs, dissipating by 5 min (**Fig. 4E and F**). In addition, SDC4 was internalized in response to VEGFA in cells HUVECS expressing an HA-tagged form of SDC4 (**Fig. 4G**). Critically, a second assay also revealed that VEGFA-induced phosphorylation of VEGFR2 was markedly decreased in *Sdc4*-/- MLECs compared to WT MLECs (**Fig. 4H**). Flow cytometry analysis of lung digests confirmed that cell surface expression of VEGFR2 was the same between WT and *Sdc4-/-* lung ECs (**fig. S10A and B**). Taken together, this data suggests that SDC4 acts to facilitate VEGFR2-mediated responses to VEGFA. This has functional implications for VEGFR2-dependent signaling pathways; one of which is the promotion of VE-Cadherin internalization leading to dissociation of cell-cell contacts in ECs (a key step in the angiogenic process[24]). To examine this, wild type MLECs were treated with VEGFA for 5 min, whereupon VE-Cadherin disappeared from cell junctions and was internalized into cytoplasmic vesicles, as reported[24] (**fig. S11A-C**).

In contrast, VE-Cadherin was retained in EC adherens junctions of *Sdc4*-/- cells following VEGFA treatment. Based on this we investigated VE-Cadherin expression in normal and OIR retinas. VE-Cadherin expression was normal in retinas at P17, but disrupted in OIR. Although normal VE-Cadherin expression was disrupted in some of the angiogenic blood vessels in *Sdc4-/-* retinas in OIR, the disruption was more severe in WT retinas. VE-Cadherin was almost totally absent from some blood vessels or was internalized in some of the vessels in WT retinas in OIR. These features were especially prominent in pre-retinal tufts that represent pathological angiogenesis in OIR (**fig. S12**). We then tested whether the decrease in VEGFR2 phosphorylation observed in *ex vivo Sdc4*-/- ECs was sufficient to affect physiological responses to VEGFA in an acute *in vivo* setting. Whereas WT and *Sdc4*-/- mice displayed similar levels of basal and bradykinin-induced vascular permeability in dorsal skin, vascular leakage induced by VEGFA was abolished in *Sdc4*-/- null mice (**Fig. 4I and J**).

2.2.5 Targeting SDC4 has therapeutic potential

Because our results suggest that VEGFA-driven angiogenesis requires the formation of a tri-molecular complex including SDC4, VEGFR2 and VEGFA on the cell surface of ECs, we tested the effect of the addition of soluble glycanated SDC4 ectodomain (solS4) to the medium of WT cells to disrupt this complex. As expected, treatment of primary MLECs with solS4 diminished the activation of VEGFR2 in response to VEGFA after 5 min (**Fig. 5A and B**). Disruption of VEGFA signaling by solS4 was also demonstrated by scratch wound cell migration assays on HUVEC monolayers. Cell migration was significantly enhanced by VEGFA treatment in control cells, but this effect was abrogated in cells treated with solS4. Consistent with our previous work we also saw inhibition of HUVEC cell migration in cells treated with soluble glycanated syndecan-2 ectodomain (solS2)[16] but, unlike with solS4, VEGFA-induced increase in cell migration was unaffected by the treatment with solS2 (**Fig. 5C)** indicating that disruption of VEGFA responses is a characteristic specific to SDC4.

We also tested solS4 in the *ex vivo* mouse aortic ring assay of neovascularization and observed a strong reduction in the angiogenic response to VEGFA (**Fig. 5D and E**). Finally, we administered solS4 to mice in the laser CNV model and compared its effects to EYLEA, a recombinant protein corresponding to the VEGFA binding portion of VEGR2. Lesion formation was greatly reduced in response to both treatments indicating the therapeutic potential of targeting syndecan-4 (**Fig. 5F and G**).

This study highlights SDC4 as a regulator of EC responses to VEGFA and loss of this molecule in disease model systems leads to greatly reduced angiogenesis (model shown in **Fig. 6**). These data highlight an important difference between angiogenic responses in disease models which require SDC4 and developmental angiogenesis in which SDC4 is not essential, based on the fact that no gross abnormalities are evident in the *Sdc4-/-* mouse. The existence of inflammation related regulatory elements (eg. NF-κB, and hypoxia response elements[25]) within the SDC4 promoter support the idea that the expression and function of this molecule is driven by responses to stress or injury. Based on our data and others it seems unlikely that there is redundancy between syndecan family members and other HSPGs during these pathological responses whereas maybe this is the case during development. Both SDC-1 and -2 have been shown to contain angiogenesis regulatory peptide sequences with their extracellular core proteins and these bear little homology to each other and act through distinct receptors. Similarly, SDC4 also contains a unique peptide sequence within its extracellular core protein and it is possible that this, in addition to the HS chains are responsible for the specificity of the interactions described here.

We show an association between SDC4 and VEGFR2 and a rapid appearance and subsequent disappearance from the cell surface of both molecules in response to VEGFA is suggestive of a role for SDC4 in the trafficking of VEGFR2. SDC4 is known to be intimately associated with trafficking of integrins, most notably α5β1, and β1 integrins are also known to complex with VEGFR2 so SDC4 may form part of a larger signaling nexus involving integrins and components of the VEGF signaling pathway.

The possibility of the involvement in this trafficking pathway of PDZ proteins, via interactions with the intracellular SDC4 C-terminus also cannot be excluded. Particularly as studies have shown a role for both syntenin and synectin (both known to bind SDC4) in VEGR2 trafficking and signaling. Furthermore, recent studies have also shown a role for SDC4 in calcium signaling and this would also be consistent with the defects in Ve-Cadherin redistribution we see after treatment with VEGFA.

In this study, we used a recombinant protein corresponding to the extracellular core protein of SDC4 produced in mammalian cells, such that the HS chains would be present on this molecule, and this blocked VEGFA induced angiogenesis in both cell-based and *in vivo* models. These results suggest that SDC4 blocking strategies could be applied in the treatment of cancer and vascular diseases where neovascularization is a factor and may either improve or offer an alternative to existing therapies. Since SDC4 only impacts neovascularization in pathological scenarios, therapeutic innovations targeting this molecule may have a more favorable side effect profile than current therapeutic options.

2.3 Figures & Legends

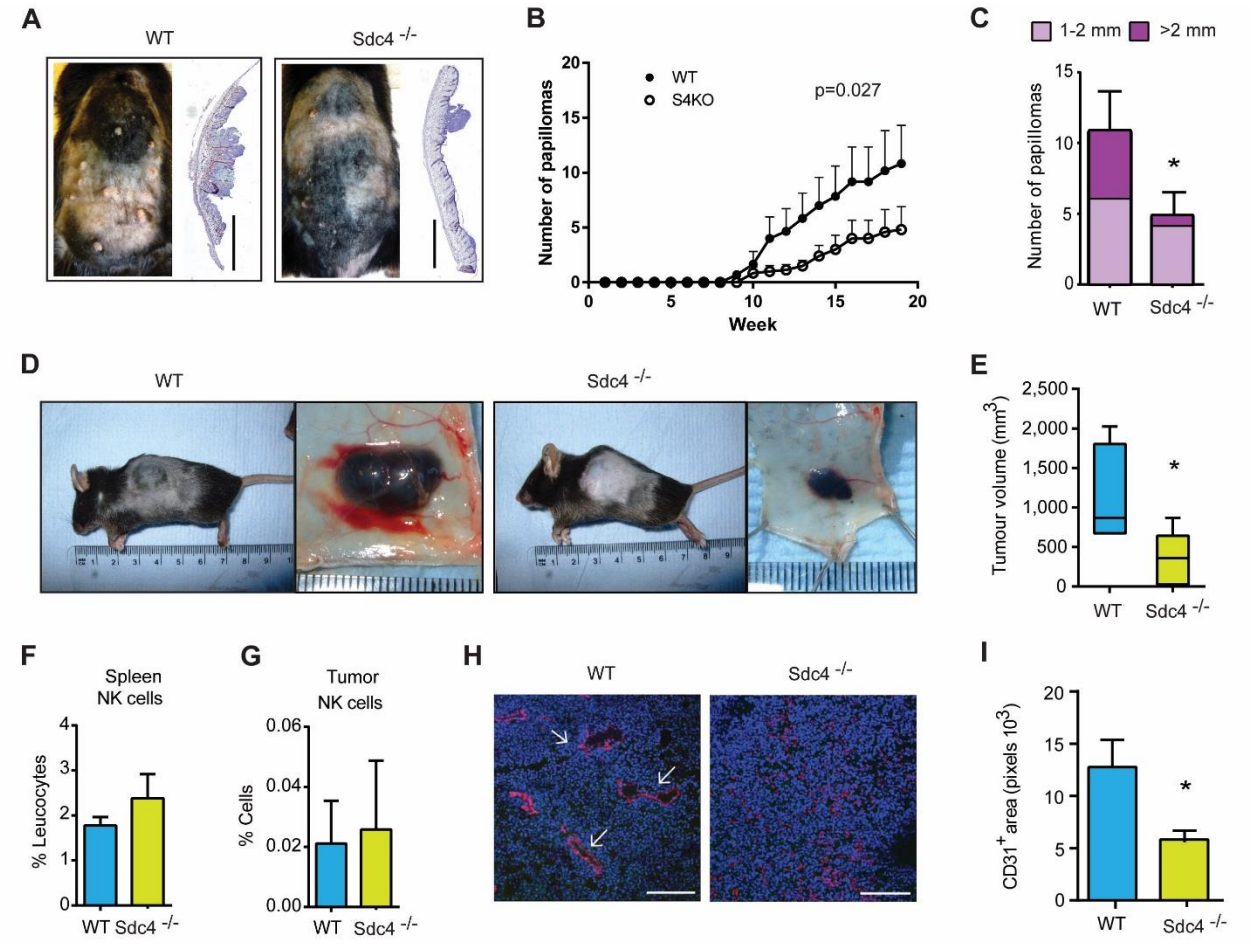

2.3.2 Figure 1: Tumor angiogenesis is impaired in *Sdc4-/-* mice.

(A) Papilloma formation is reduced in *Sdc4-/-* mice in the DBMA/TPA model. Micrographs of animals (left) and sections of skin (right, H&E) from WT and *Sdc4-/-* animals at week 19 (scale bar = 2 mm). **(B)** Number of large tumors (≥2 mm/mouse) over time and **(C)** size of papillomas at end of the experiment (n=7 mice/group). **(D)** Micrographs of B16F0 melanomas from WT and *Sdc4-/-* animals showing reduced tumor volume as quantified in **(E)** (n=5-6 mice/group). Levels of NK cells are equal in WT and *Sdc4-/-* animals in both spleen **(F)** and B16F0 tumor immune infiltrates **(G)** (n=3 mice/group). **(H)** Tumor vessels (arrowheads) appear in WT sections but are not obvious in B16F0 melanomas from *Sdc4-/-* mice (Ki-67, blue; CD31 red, scale bar = 100 µM), **(I)** quantification of tumor vessel coverage (n=5/group, 3 images/animal). *P < 0.05. Error bars indicate SEM.

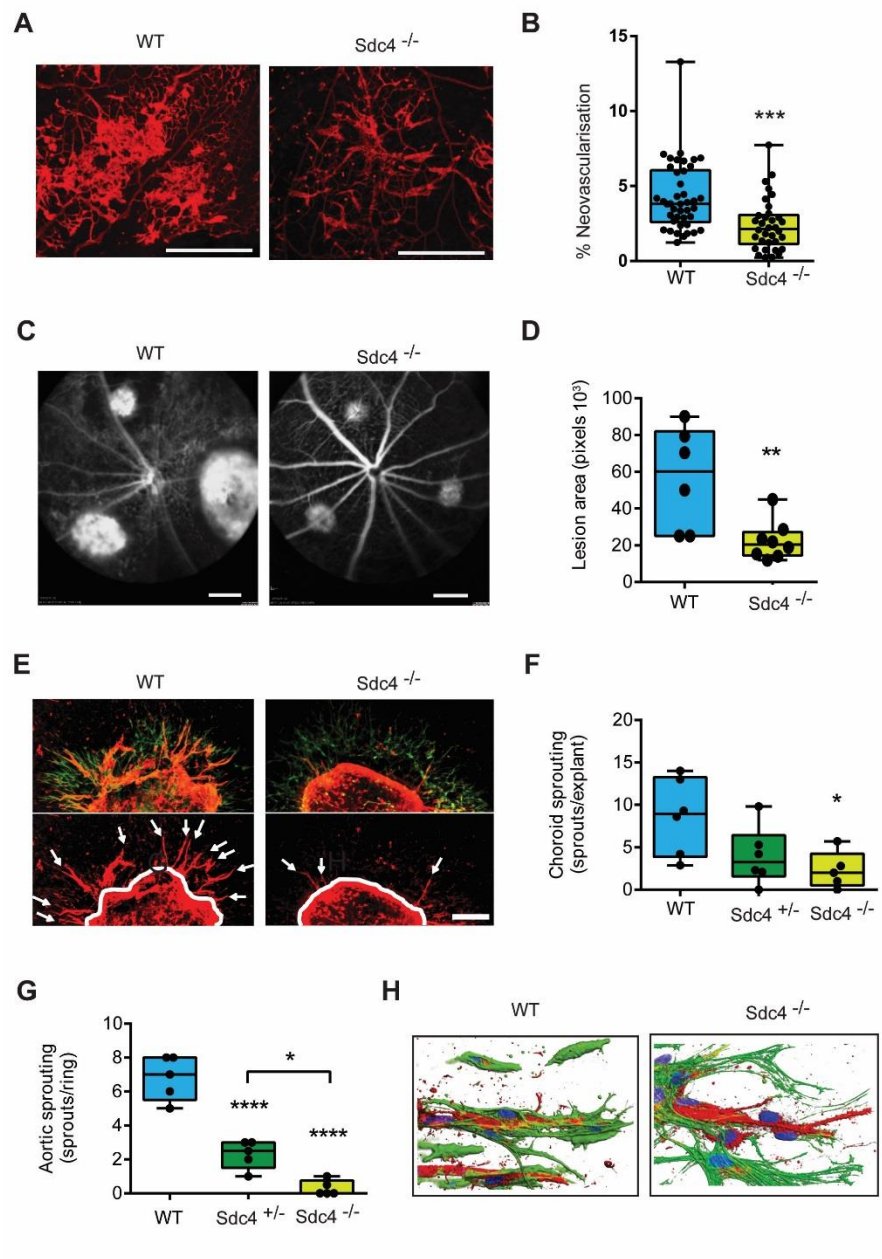

2.3.2 Figure 2: Pathological neovascularization is impaired in *Sdc4-/-* animals.

(A) Micrographs showing the pre-retinal neovascularization response (stained with BS1-isolectin) to OIR in P17 WT neonates is greater than in equivalent *Sdc4-/-* animals (Scale bar = 500 µM). **(B)** Quantification of pre-retinal neovascularization (~40 eyes/group). **(C)** Micrographs showing *Sdc4-/-* animals exhibit less angiogenesis in the laser induced CNV model as evident from reduced lesion area **(D)** (n=6-8 animals/group, Scale bar = 2.4 mm). **(E)** Angiogenic sprouting is reduced in *Sdc4-/-* choroid explants, stained with BS1-Isolectin (red) and anti-αSMA (green) after 7 days in culture (Scale bar = 10 µM). Gene-dosage effect between WT, *Sdc4+/-* and *Sdc4-/-*

(F) choroid and **(G)** aortic explants (n=5-6 animals/group). **(H)** Micrographs of aortic ring angiogenic sprouts showing reduced pericyte coverage on sprouts from *Sdc4-/-* rings (CD31: red, DAPI: blue, αSMA: green, Scale bar = 20 μm). *P < 0.05; **P < 0.01; ***P<0.001; ****P<0.0001. Error bars indicate min and max values.

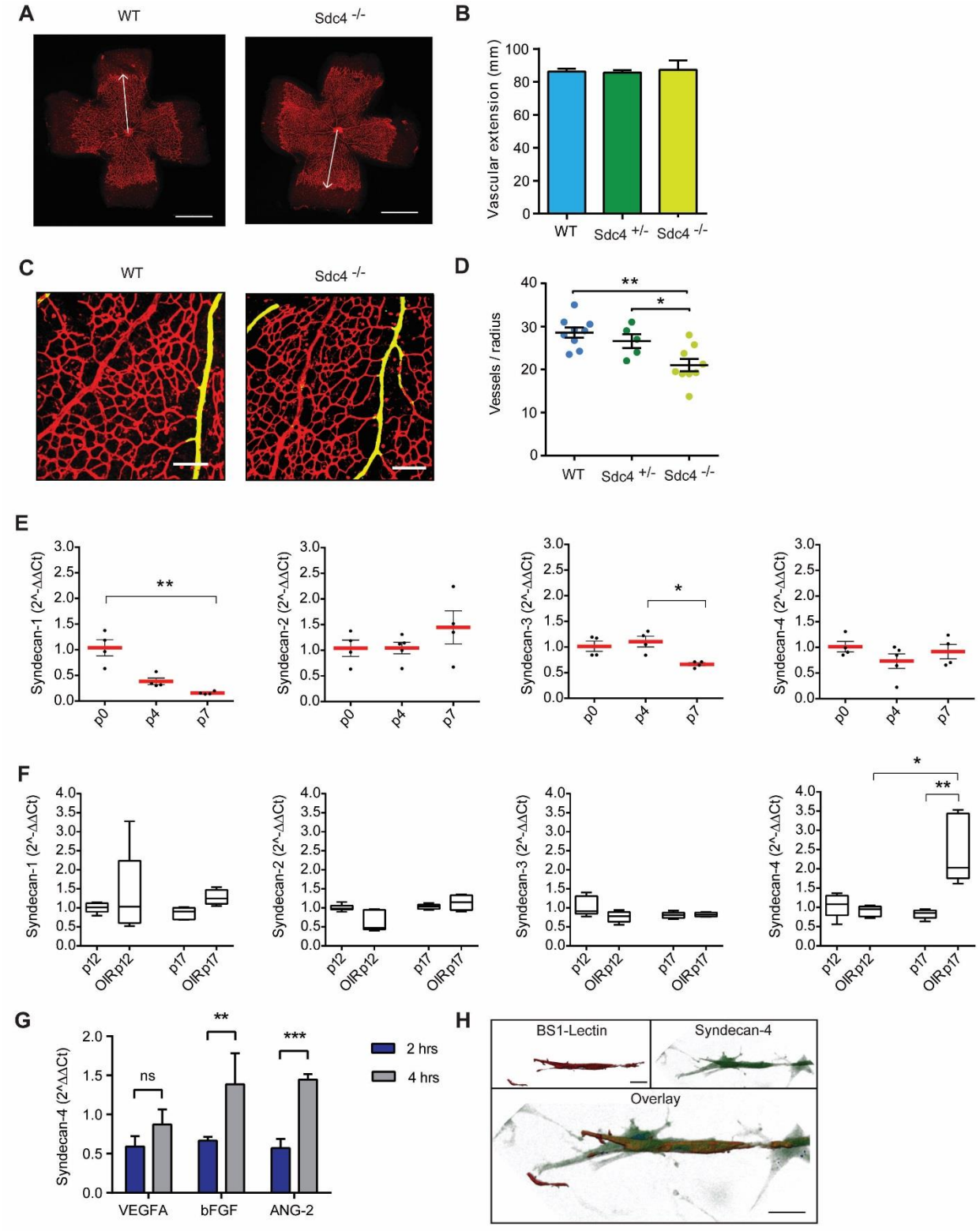

2.3.3 Figure 3: SDC4 expression is upregulated during pathological angiogenesis.

(A) Retinas from P6 WT and *Sdc4-/-* neonates stained with BS1-isolectin (Scale bar = 1 mm). **(**B**)** Vascular extension as shown by arrows in **(A)** is the same in WT, *Sdc4+/-* and *Sdc4-/-* animals (n=10-15 animal/genotype). **(C)** Magnified images of retinal vasculature (Scale bar: 100 μm) and **(D)** the number of vessels along a given radius is slightly reduced in the absence of SDC4. **(E)** Syndecan gene expression profile during early stages of murine retinal angiogenesis. SDC4 expression remains unchanged (n=5-6) across the time course. **(F)** OIR induces syndecan-4 expression at day 17. Syndecan gene expression in neonates after OIR as compared to untreated controls. Syndecan-4 gene expression is significantly increased on day P17 in OIR treated animals. **(G)** SDC4 gene expression increases in response to VEGFA, bFGF and ANG-2 in MLECs (n=3). **(H)** SDC4 (green) is expressed on ECs (red) on angiogenic sprouts from aortic rings (Scale bar = 200 μm). *P < 0.05; **P < 0.01; ***P<0.001. Error bars indicate SEM in B, D, E and G and min and max values in F.

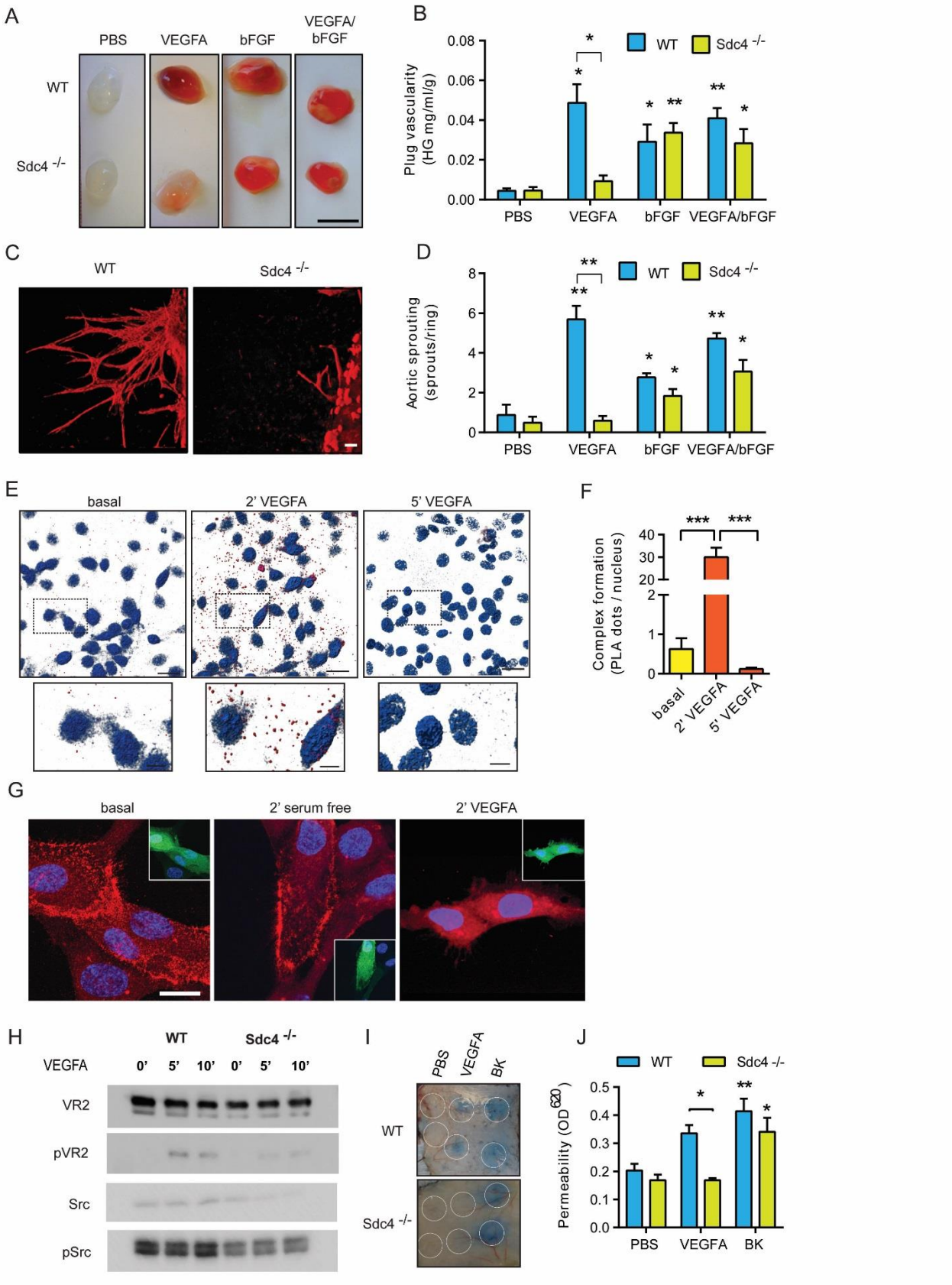
A
PBS
VEGFA
bFGF
VEGFA/
bFGF
WT
Sdc4 -/-
B
Plug vascularity
(HG mg/ml/g)
0.08
0.06
0.04
0.02
0.00
WT
Sdc4 -/-
PBS
VEGFA
bFGF
VEGFA/bFGF
C
WT
Sdc4 -/-
D
Aortic sprouting
(sprouts/ring)
8
6
4
2
0
WT
Sdc4 -/-
PBS
VEGFA
bFGF
VEGFA/bFGF
E
basal
2' VEGFA
5' VEGFA
F
Complex formation
(PLA dots / nucleus)
40
30
20
2
1
0
basal
2' VEGFA
5' VEGFA
G
basal
2' serum free
2' VEGFA
H
WT
Sdc4 -/-
VEGFA
0'
5'
10'
0'
5'
10'
VR2
pVR2
Src
pSrc
I
PBS
VEGFA
BK
WT
Sdc4 -/-
J
WT
Sdc4 -/-
Permeability (OD620)
0.5
0.4
0.3
0.2
0.1
0.0
PBS
VEGFA
BK

2.3.4 Figure 4: Defective angiogenesis in *Sdc4-/-* mice is due to a lack of responsiveness to VEGFA.

(A and B) Matrigel plugs and **(C and D)** aortic rings supplemented with bFGF and VEGFA alone or in combination reveal *Sdc4-/-* tissues fail to respond to VEGFA alone (n=6/condition). **(E)** Proximity ligation assays show that SDC4 and VEGFR2 interact after treatment with VEGFA (Scale bar: 20 µm, 7 µm). **(F)** Quantification of PLA experiments was performed using ImageJ software (n=3, 7 images per condition). **(G)** Syndecan-4 is internalized in HUVECs after treatment with VEGFA (10 ng/ml) at the times indicated (Scale bar 20 µm). **(H)** Impaired VEGFR2 phosphorylation in Sdc4-/- MLECs. **(I and J)** Miles assay showing that VEGFA induced vascular permeability is impaired in *Sdc4-/-* mice (n=6-9 animals/group). *P < 0.05; **P < 0.01; ***P<0.001. Error bars indicate SEM. Comparisons made between treatments and PBS are within the same genotype unless otherwise indicated (bar).

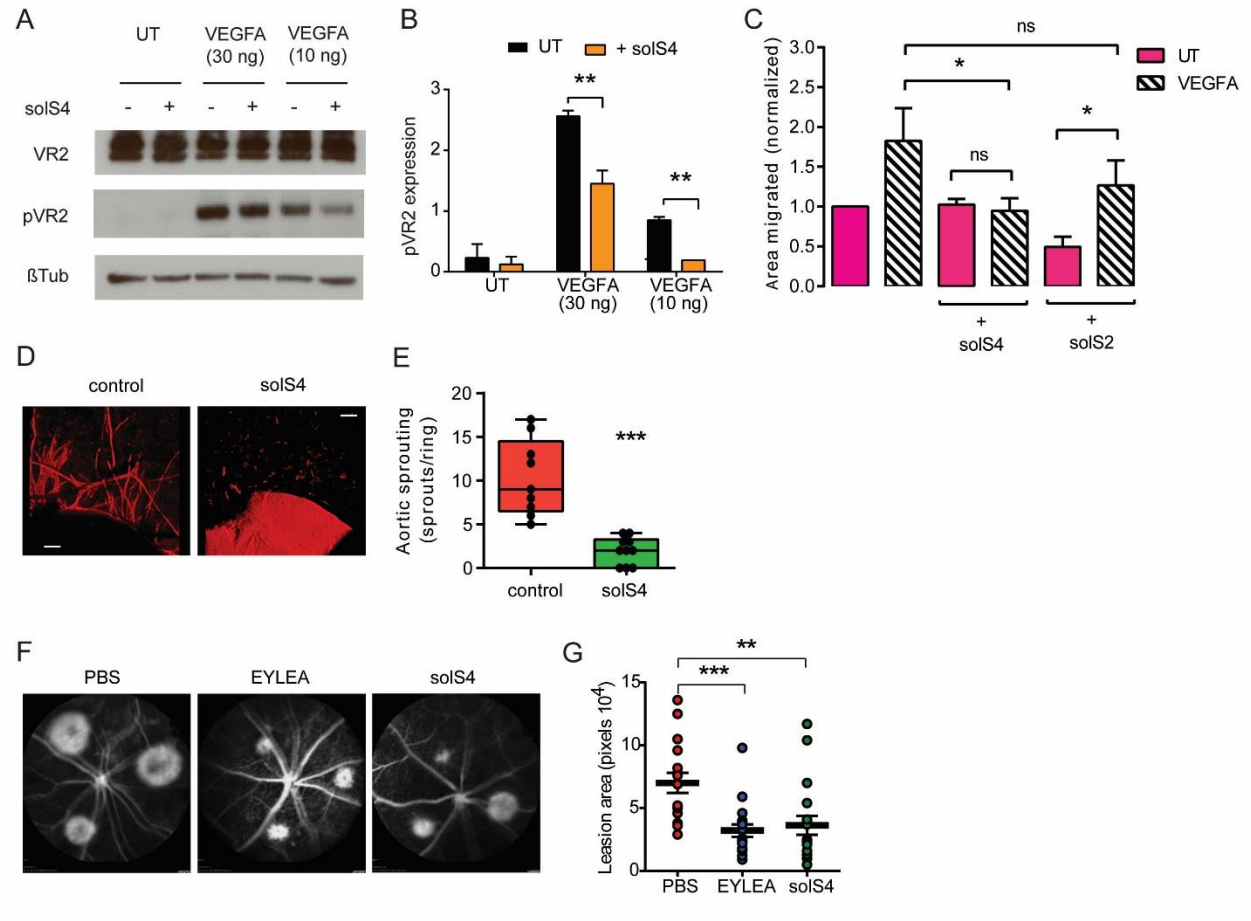

2.3.5 Figure 5: Therapeutic potential of targeting syndecan-4 to block VEGFA induced pathological angiogenesis.

(A and B) Soluble SDC4 ectodomain (solS4, 10 µg) inhibits VEGFR2 phosphorylation in response to VEGFA in HUVECS. **(C)** VEGFA-induced EC migration is inhibited in the presence of solS4 but not solS2. **(D and E)** Soluble SDC4 ectodomain inhibits VEGFA induced angiogenic sprout formation in a rat aortic ring assay (n=4, 5-15 rings/condition). **(F and G)** SolS4 inhibits lesion formation in response to Laser induced CNV and its effects compare favorably to Eylea (n=6-8 animals). *P < 0.05; **P < 0.01; ***P<0.001. Error bars indicate SEM in B, C and G and min and max values in E.

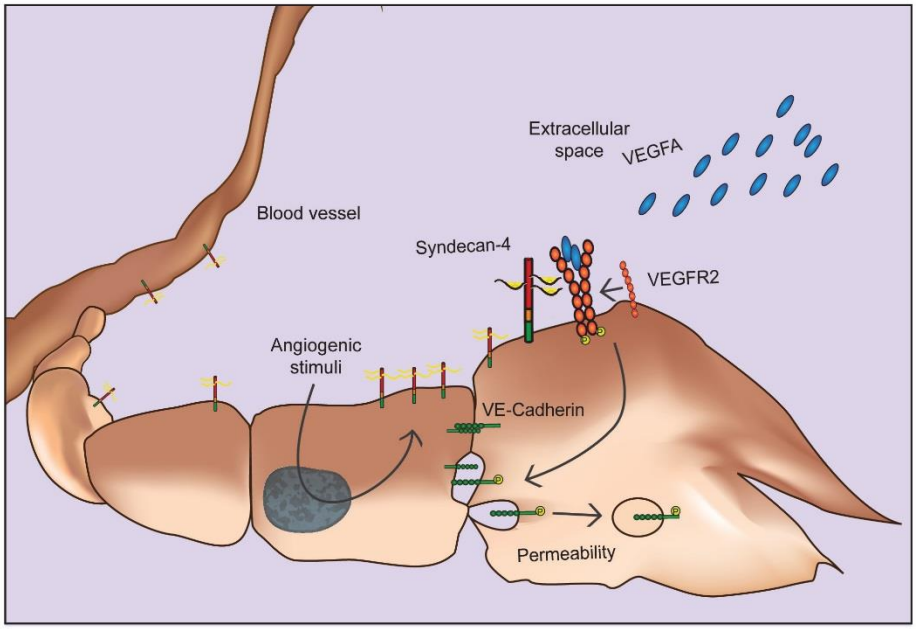

2.3.6 Figure 6: Syndecan-4 is involved in VEGFA signaling response during pathological angiogenesis.

2.4 References

1. Eming SA, Martin P and Tomic-Canic M. Wound repair and regeneration: Mechanisms, signaling, and translation. *Science Translational Medicine*. 2014;6.
2. Jayson GC, Kerbel R, Ellis LM and Harris AL. Antiangiogenic therapy in oncology: current status and future directions. *Lancet*. 2016;388:518-529.
3. Amadio M, Govoni S and Pascale A. Targeting VEGF in eye neovascularization: What's new? A comprehensive review on current therapies and oligonucleotide-based interventions under development. *Pharmacological Research*. 2016;103:253-269.
4. Carmeliet P and Jain RK. Molecular mechanisms and clinical applications of angiogenesis. *Nature*. 2011;473:298-307.
5. Adams RH and Alitalo K. Molecular regulation of angiogenesis and lymphangiogenesis. *Nature reviews Molecular cell biology*. 2007;8:464-78.
6. Meadows KL and Hurwitz HI. Anti-VEGF therapies in the clinic. *Cold Spring Harbor perspectives in medicine*. 2012;2.
7. Kurihara T, Westenskow PD, Bravo S, Aguilar E and Friedlander M. Targeted deletion of Vegfa in adult mice induces vision loss. *Journal of Clinical Investigation*. 2012;122:4213-4217.
8. Couchman JR. Transmembrane signaling proteoglycans. *Annu Rev Cell Dev Biol*. 2010;26:89-114.
9. Hacker U, Nybakken K and Perrimon N. Heparan sulphate proteoglycans: The sweet side of development. *Nature Reviews Molecular Cell Biology*. 2005;6:530-541.

10. Robinson CJ, Mulloy B, Gallagher JT and Stringer SE. VEGF(165)-binding sites within heparan sulfate encompass two highly sulfated domains and can be liberated by K5 lyase. *Journal of Biological Chemistry*. 2006;281:1731-1740.
11. Ashikari- Hada S, Habuchi H, Kariya Y and Kimata K. Heparin regulates vascular endothelial growth factor(165)-dependent mitogenic activity, tube formation, and its receptor phosphorylation of human endothelial cells - Comparison of the effects of heparin and modified heparins. *Journal of Biological Chemistry*. 2005;280:31508-31515.
12. Nishiguchi KM, Kataoka K, Kachi S, Komeima K and Terasaki H. Regulation of Pathologic Retinal Angiogenesis in Mice and Inhibition of VEGF-VEGFR2 Binding by Soluble Heparan Sulfate. *PloS one*. 2010;5.
13. Okina E, Manon-Jensen T, Whiteford JR and Couchman JR. Syndecan proteoglycan contributions to cytoskeletal organization and contractility. *Scandinavian Journal of Medicine & Science in Sports*. 2009;19:479-489.
14. Elfenbein A and Simons M. Syndecan-4 signaling at a glance. *Journal of Cell Science*. 2013;126:3799-3804.
15. De Rossi G and Whiteford JR. Syndecans in angiogenesis and endothelial cell biology. *Biochemical Society transactions*. 2014;42:1643-6.
16. De Rossi G, Evans AR, Kay E, Woodfin A, McKay TR, Nourshargh S and Whiteford JR. Shed syndecan-2 inhibits angiogenesis. *Journal of cell science*. 2014.
17. Beauvais DM, Ell BJ, McWhorter AR and Rapraeger AC. Syndecan-1 regulates alphavbeta3 and alphavbeta5 integrin activation during angiogenesis and is blocked by synstatin, a novel peptide inhibitor. *The Journal of experimental medicine*. 2009;206:691-705.
18. Echtermeyer F, Streit M, Wilcox-Adelman S, Saoncella S, Denhez F, Detmar M and Goetinck P. Delayed wound repair and impaired angiogenesis in mice lacking syndecan-4. *The Journal of clinical investigation*. 2001;107:R9-R14.

19. Ishiguro K, Kadomatsu K, Kojima T, Muramatsu H, Nakamura E, Ito M, Nagasaka T, Kobayashi H, Kusugami K, Saito H and Muramatsu T. Syndecan-4 deficiency impairs the fetal vessels in the placental labyrinth. *Developmental dynamics : an official publication of the American Association of Anatomists*. 2000;219:539-44.
20. Jain RK. Antiangiogenesis Strategies Revisited: From Starving Tumors to Alleviating Hypoxia. *Cancer Cell*. 2014;26:605-622.
21. El Ghazal R, Yin X, Johns SC, Swanson L, Macal M, Ghosh P, Zuniga EI and Fuster MM. Glycan Sulfation Modulates Dendritic Cell Biology and Tumor Growth. *Neoplasia (New York, NY)*. 2016;18:294-306.
22. Grossniklaus HE, Kang SJ and Berglin L. Animal models of choroidal and retinal neovascularization. *Progress in Retinal and Eye Research*. 2010;29:500-519.
23. Prewett M, Huber J, Li YW, Santiago A, O'Connor W, King K, Overholser J, Hooper A, Pytowski B, Witte L, Bohlen P and Hicklin DJ. Antivascular endothelial growth factor receptor (fetal liver kinase 1) monoclonal antibody inhibits tumor angiogenesis and growth of several mouse and human tumors. *Cancer Research*. 1999;59:5209-5218.
24. Gavard J and Gutkind JS. VEGF controls endothelial-cell permeability by promoting the beta-arrestin-dependent endocytosis of VE-cadherin. *Nature Cell Biology*. 2006;8:1223-U17.
25. Fujita N, Hirose Y, Tran CM, Chiba K, Miyamoto T, Toyama Y, Shapiro IM and Risbud MV. HIF-1-PHD2 axis controls expression of syndecan 4 in nucleus pulposus cells. *FASEB journal : official publication of the Federation of American Societies for Experimental Biology*. 2014;28:2455-65.